International Journal of Advance Research Publication and Reviews

Vol 03, Issue 10, pp 246-258, October, 2026

Event-Based Analysis of Forbush Decreases and Associated Solar Wind and Geomagnetic Disturbances During Solar Cycle 24

Prerana Singh[1], Dr. Mukta Tripathi[2]

[1]Research Scholar, Department of Physics, A.P.S. University Rewa (M.P.), India

[2]Assistant Professor, Department of Physics, A.P.S. University Rewa (M.P.) India

ABSTRACT

Forbush decreases (FDs) are short-term reductions in the intensity of galactic cosmic rays observed near Earth following disturbances propagating through the heliosphere. These variations provide useful information about the interaction between solar-transient structures, the interplanetary medium, and cosmic-ray transport. The present study investigates individual Forbush decrease events during Solar Cycle 24 with particular emphasis on their association with solar-wind conditions and geomagnetic disturbances. The study considers the temporal behaviour of cosmic-ray intensity together with selected solar-wind and geomagnetic parameters, including solar-wind speed, interplanetary magnetic field strength and its north–south component, solar-wind plasma density, Dst, Kp, and Ap indices. Coronal mass ejection information is also considered to identify possible solar and interplanetary sources associated with the observed events.

The analysis follows an event-based approach in which significant decreases in cosmic-ray intensity are identified and characterized in terms of their onset, magnitude, duration, minimum intensity, and recovery behaviour. The corresponding solar-wind and geomagnetic conditions are examined around each selected event to determine the interrelationship between cosmic-ray modulation and interplanetary disturbances. Statistical techniques, including correlation analysis and comparative event analysis, are employed to examine the association between Forbush decrease characteristics and variations in solar-wind and geomagnetic parameters. Graphical representations and event-wise data tables are used to illustrate the temporal evolution and relationships among the investigated parameters.

The study is restricted to Solar Cycle 24, thereby providing a consistent framework for examining Forbush decreases during a single complete solar cycle. The results are expected to contribute to a better understanding of the interplanetary conditions associated with cosmic-ray decreases and their simultaneous geomagnetic responses. The investigation also provides an observational basis for understanding solar–terrestrial coupling and the role of transient solar-wind disturbances in modulating near-Earth cosmic-ray intensity.

Keywords: Forbush decrease; cosmic rays; Solar Cycle 24; solar wind; interplanetary magnetic field; geomagnetic activity; Dst; Kp; Ap; coronal mass ejection.

1. Introduction

The Sun is the principal source of energy and the dominant driver of the space environment surrounding Earth. Its continuously changing magnetic activity produces variations in radiation, plasma flows, magnetic fields, and energetic particles throughout the heliosphere. These changes can influence the propagation of charged particles and can ultimately affect the near-Earth space environment. The interaction between solar activity, the interplanetary medium, cosmic rays, and the terrestrial magnetic field is therefore an important component of solar-terrestrial physics and space-weather research (Pomerantz, 1974; Potgieter, 2013).

Galactic cosmic rays (GCRs) are highly energetic charged particles that enter the heliosphere from sources beyond the solar system. During their propagation toward the inner heliosphere, these particles are affected by the solar wind and the interplanetary magnetic field (IMF). Their transport involves several processes, including diffusion, convection, energy changes, and particle drift. Consequently, the intensity of cosmic rays observed near Earth does not remain constant but changes in response to variations in heliospheric conditions. Long-term changes are related to solar-cycle modulation, whereas transient disturbances in the solar wind can produce comparatively rapid changes in cosmic-ray intensity (Potgieter, 2013; Adhikari et al., 2022).

One of the most significant short-term variations in GCR intensity is the Forbush decrease (FD). It is generally observed as a temporary reduction in cosmic-ray intensity followed by a more gradual recovery toward the background level. The phenomenon was first identified in systematic cosmic-ray observations in the early twentieth century and subsequently became an important indicator of transient disturbances in interplanetary space. FDs can be detected using ground-based neutron monitors as well as other cosmic-ray instruments. Their characteristics provide information about the interaction between energetic particles and disturbed magnetic structures propagating through the heliosphere (Cane, 2000; Richardson & Cane, 2011).

The occurrence of an FD is frequently associated with interplanetary coronal mass ejections (ICMEs), although other solar-wind structures, particularly corotating interaction regions (CIRs), can also produce cosmic-ray decreases. An ICME can contain an enhanced and relatively ordered magnetic field, while the region ahead of it may contain a turbulent sheath generated by the interaction between the disturbance and the ambient solar wind. These magnetic and turbulent structures can reduce the access and transport of GCRs through the disturbed region. Consequently, the cosmic-ray decrease observed near Earth may reflect the combined influence of the sheath and the magnetic structure associated with the ICME rather than a single physical component (Cane, 2000; Richardson & Cane, 2011).

The magnitude and temporal profile of an FD are not necessarily the same for different events. Important characteristics include the onset time, percentage decrease, minimum intensity, duration, and recovery period. The recovery phase may also exhibit dependence on particle energy, indicating that cosmic-ray transport during the recovery interval is influenced by particle rigidity and the properties of the surrounding magnetic field (Usoskin et al., 2008). Such differences make event-based analysis particularly useful because averaging a large number of events may obscure the physical characteristics of individual disturbances.

Solar-wind parameters provide important information for interpreting these variations. An increase in solar-wind speed, enhancement of the IMF magnitude, and changes in the magnetic-field orientation can accompany the arrival of an interplanetary disturbance at Earth. The structure of the shock, sheath, and ICME can therefore be examined in relation to the observed cosmic-ray response. Previous investigations have shown that the magnitude of some FDs is related to properties such as CME speed, the maximum solar-wind speed, and the characteristics of the associated interplanetary magnetic structure (Belov et al., 2014).

The geomagnetic response provides another important component of the solar-terrestrial connection. When an interplanetary disturbance reaches Earth, its magnetic field can interact strongly with the terrestrial magnetosphere. The southward component of the IMF, particularly the GSM (B_z) component, can enhance magnetic reconnection at the dayside magnetopause and contribute to increased geomagnetic activity. Consequently, solar-wind disturbances responsible for FDs may also be accompanied by changes in geomagnetic indices. Studies of magnetic clouds and their surrounding sheath regions have demonstrated that the magnetic structures responsible for cosmic-ray depressions and those responsible for geomagnetic-storm development can occur within closely related parts of the same interplanetary disturbance (Huttunen et al., 2002).

Several geomagnetic indices can be used to quantify this response. The disturbance storm time (Dst) index is commonly used to characterize the intensity of the storm-time disturbance associated mainly with the equatorial ring current. The planetary Kp index provides a measure of global geomagnetic activity, while Ap is a linearized representation derived from Kp and is useful for statistical analysis. Considering these indices together with solar-wind and IMF parameters allows the geomagnetic consequences of individual FD-associated disturbances to be examined more systematically.

Solar Cycle 24 provides a particularly useful period for investigating these relationships. The cycle began after a prolonged solar minimum and was generally characterized by relatively low sunspot activity compared with several preceding solar cycles. Nevertheless, significant solar eruptions and interplanetary disturbances occurred throughout the cycle. Investigations of Solar Cycle 24 have shown that its geomagnetic environment had distinctive characteristics, including a reduction in the occurrence of intense geomagnetic storms compared with Solar Cycle 23, while moderate disturbances remained important (Selvakumaran et al., 2016).

The presence of significant transient activity during an otherwise comparatively weak solar cycle is particularly relevant to FD research. For example, the September 2017 solar-activity episode during the declining phase of Solar Cycle 24 produced several powerful flares, halo CMEs, energetic-particle events, geomagnetic disturbances, and observable decreases in galactic cosmic rays. This demonstrates that a relatively weak solar cycle can nevertheless contain individual events capable of producing substantial solar-terrestrial effects (Chertok et al., 2018).

Previous investigations have established the close relationship between CMEs, interplanetary magnetic structures, cosmic-ray decreases, and geomagnetic disturbances. However, individual FD events can differ considerably in their intensity, temporal evolution, solar-wind characteristics, and geomagnetic response. A detailed event-based approach is therefore useful for examining these differences rather than treating all disturbances as a single homogeneous population. Such an approach can also help identify whether stronger cosmic-ray depressions systematically occur with particular solar-wind or geomagnetic conditions.

The present study focuses specifically on the event-based analysis of Forbush decreases and associated solar-wind and geomagnetic disturbances during Solar Cycle 24. The analysis considers cosmic-ray intensity variations together with relevant solar-wind and geomagnetic parameters. Parameters such as solar-wind speed, IMF characteristics, (B_z), Dst, Kp, and Ap are examined to investigate the conditions accompanying selected FD events. CME observations are additionally considered to establish the possible association between individual cosmic-ray decreases and solar-origin disturbances.

The principal objective is to characterize FD events during Solar Cycle 24 and investigate their association with interplanetary and geomagnetic

conditions. Particular emphasis is placed on the temporal behavior of individual events, their magnitude and duration, the accompanying solar-wind disturbances, and the corresponding geomagnetic response. Comparative examination of individual events is intended to identify common characteristics as well as event-to-event differences.

By combining cosmic-ray observations with solar-wind, CME, and geomagnetic information, this study seeks to provide a systematic description of the sequence connecting solar eruptions, interplanetary disturbances, cosmic-ray modulation, and geomagnetic activity. The resulting analysis can contribute to a clearer understanding of transient solar-terrestrial coupling during Solar Cycle 24 and can help demonstrate the usefulness of cosmic-ray observations as an additional indicator of disturbed heliospheric conditions.

2. Literature Review

Forbush decreases have been investigated for many decades as an important manifestation of the interaction between solar disturbances, the interplanetary magnetic field, and galactic cosmic rays. The phenomenon was first recognized through the observation that cosmic-ray intensity could decrease substantially during periods of geomagnetic disturbance. Subsequent observations established that these decreases were associated with disturbances propagating through interplanetary space rather than being produced solely within the terrestrial atmosphere. Early theoretical and observational studies consequently established the foundation for interpreting Forbush decreases as a solar-terrestrial phenomenon (Forbush, 1937; Simpson, 1954; Cane, 2000).

One of the important developments in FD research was the recognition that different portions of an interplanetary disturbance can contribute to the observed cosmic-ray reduction. Cane (2000) reviewed the relationship between cosmic-ray decreases and interplanetary disturbances and emphasized the importance of shocks, turbulent sheath regions, and magnetic ejecta. According to this framework, enhanced magnetic turbulence can inhibit the transport of cosmic rays, while strong magnetic structures associated with interplanetary coronal mass ejections (ICMEs) can produce additional modulation. Thus, the observed FD profile may represent the combined effect of several structures within a solar-wind disturbance rather than a response to a single physical region.

The association between ICMEs and cosmic-ray decreases was subsequently examined using large event samples. Richardson and Cane (2011) investigated more than 300 ICMEs and their associated shocks observed near Earth during 1995–2009. Their analysis showed that a decrease in galactic cosmic-ray intensity occurred during approximately four-fifths of the investigated ICME passages. For events exhibiting a decrease, the minimum cosmic-ray intensity was commonly reached while the ICME itself was passing the observing location. Their results therefore supported the important roles of both the post-shock region and the ICME in producing FD signatures.

The internal structure of FDs has also received considerable attention. Jordan et al. (2011) examined whether the traditional two-step FD model could consistently explain observations associated with ICMEs and their shocks. Using neutron-monitor observations together with spacecraft measurements, they found that only a relatively small fraction of the examined ICME events displayed a clear two-step profile. Their findings indicated that FD profiles can be considerably more complex than the simplified two-component model suggests and that smaller-scale magnetic structures within the interplanetary medium can influence the observed cosmic-ray response.

Another important aspect of FD research concerns the distinction between CME-driven events and recurrent solar-wind disturbances. Not all cosmic-ray decreases require a direct encounter with an ICME. Corotating interaction regions (CIRs), produced when fast solar-wind streams interact with slower surrounding plasma, can also modulate cosmic rays. Studies have therefore emphasized that the magnitude and temporal profile of an FD depend on the type and structure of the interplanetary disturbance encountered by Earth. Algorithm-based investigations have similarly noted differences between larger, CME-related decreases and smaller events associated with other solar-wind structures (Cane, 2000; Belov et al., 2001).

Statistical investigations have further demonstrated that the amplitude of an FD cannot be interpreted independently of the characteristics of the associated solar-wind disturbance. Solar-wind velocity, IMF strength, turbulence, and the structure of the interplanetary magnetic field can all influence the transport of cosmic rays. The relationship is therefore not necessarily linear for every individual event. This provides a strong justification for combining event identification with comparative analysis of solar-wind and geomagnetic parameters rather than relying exclusively on long-term averages.

Solar Cycle 24 has received particular attention because of its relatively low overall level of solar activity and its unusual distribution of active periods. Lingri et al. (2017) investigated FDs during the deep minimum and mini-maximum phases of Solar Cycle 24 using a large set of events obtained from the IZMIRAN Forbush-effect database. Their study covered January 2008 to December 2014 and included 749 FD events identified from worldwide neutron-monitor observations. They examined the relationship between FD amplitude and solar as well as geomagnetic parameters, demonstrating the usefulness of Solar Cycle 24 for statistical investigations of cosmic-ray modulation.

The Solar Cycle 24 period also provides examples of major individual solar disturbances against a background of comparatively weak overall solar activity. Chertok et al. (2018) investigated the exceptional solar activity of September 2017 associated with active region AR12673. Despite the generally weak character of Solar Cycle 24, this interval produced several powerful flares and halo CMEs and was followed by solar energetic particle events, geomagnetic disturbances, and observable Forbush decreases. This event demonstrates that the average strength of a solar cycle does not necessarily determine the characteristics of every individual solar-terrestrial disturbance.

Research on geomagnetic storms has provided another important perspective on FD events. Cosmic-ray modulation and geomagnetic activity can occur during the passage of the same interplanetary disturbance, although their physical responses are not identical. Geomagnetic indices such as Dst and Kp provide information about the terrestrial response, whereas the cosmic-ray intensity records the modulation of energetic particles in interplanetary space. Consequently, examining FD magnitude together with geomagnetic indices can help identify whether stronger cosmic-ray reductions tend to occur during stronger geomagnetic disturbances.

Studies of intense Solar Cycle 24 storms have illustrated this connection. Investigations of major events, including the March 2015 geomagnetic storm, have examined cosmic-ray variations alongside solar-wind and geomagnetic parameters. Spectral studies of selected Solar Cycle 24 storms have shown that cosmic-ray intensity variations can be resolved at different time scales and that the observed FD profile changes during different phases of a geomagnetic disturbance. Such work supports the use of combined cosmic-ray, solar-wind, and geomagnetic observations when studying individual events.

More recent studies have also examined the relationship between extreme geomagnetic storms and FD profiles. Ghag et al. (2023) investigated 31 extreme geomagnetic-storm events and reported that the cosmic-ray decrease profile can be influenced by the development of the geomagnetic storm, with particularly strong relationships appearing during some phases of the disturbance. Their work reinforces the view that FD and geomagnetic responses, although physically distinct, may be strongly connected through their common interplanetary drivers.

The interaction between successive solar-wind disturbances introduces an additional level of complexity. Dumbović et al. (2022) investigated paired interacting disturbances, including successive CMEs and combinations involving high-speed streams. Their results indicated that interaction between disturbances can modify both the interplanetary magnetic field and solar-wind velocity and can influence the magnitude of the subsequent FD and geomagnetic response. This finding is important for event-based studies because an observed FD may sometimes be affected by the preceding solar-wind structure rather than representing the response to an isolated event.

Research specifically addressing strong FDs during Solar Cycle 24 has also reported an association between cosmic-ray decreases and geomagnetic indices. Pandey and Pandey (2024), for example, examined FD events with magnitudes of at least 4% during 2008–2019 and reported 19 such events. Their analysis considered Kp, Dst, and Ap in relation to FD magnitude. The study illustrates the value of combining cosmic-ray and geomagnetic observations when examining significant FD events during the complete Solar Cycle 24 period.

Overall, the existing literature establishes several important points. First, FDs are closely associated with transient disturbances in the heliosphere, particularly ICMEs and their associated shocks. Second, the cosmic-ray response can be influenced by both turbulent sheath regions and magnetic ejecta. Third, CIRs and interacting solar-wind structures can also contribute to cosmic-ray decreases. Fourth, geomagnetic activity and FD development can be related because both responses may originate from the same interplanetary disturbance. Finally, Solar Cycle 24 offers a useful natural laboratory because it combines relatively low overall solar activity with several significant individual solar eruptions and interplanetary disturbances.

Despite the extensive literature, individual FD events can differ substantially in their amplitude, duration, recovery characteristics, solar-wind conditions, and geomagnetic response. Consequently, a systematic event-based analysis using a common set of solar-wind, CME, cosmic-ray, and geomagnetic parameters remains valuable. The present study addresses this aspect by concentrating exclusively on Solar Cycle 24 and examining individual FD events in relation to their associated interplanetary and geomagnetic conditions. This approach is intended to complement earlier statistical studies by providing an integrated event-level assessment of cosmic-ray modulation and solar-terrestrial disturbances.

3. METHODOLOGY

The present study follows an event-based quantitative approach to investigate Forbush Decreases (FDs) and their association with solar-wind disturbances, interplanetary magnetic field (IMF) variations, coronal mass ejections (CMEs), and geomagnetic activity during Solar Cycle 24. The analysis is restricted to the period of Solar Cycle 24, approximately from 2008 to 2019. Cosmic-ray observations are examined together with solar-wind, IMF, CME, and geomagnetic parameters to characterize individual FD events and to investigate the associated solar-terrestrial disturbances.

The methodology involves the identification and measurement of FD events, analysis of solar-wind and IMF conditions, identification of possible CME associations, examination of geomagnetic activity, and statistical analysis of the relationships among the selected parameters. Graphical methods are also used to present the temporal and statistical relationships observed in the data.

3.1 Research Design

An event-based research design has been adopted for the present investigation. In this approach, each identified Forbush Decrease is treated as an individual event and is examined in relation to the solar and interplanetary conditions occurring before, during, and after the event.

The analysis begins with the identification of a temporary decrease in cosmic-ray intensity followed by a recovery towards the pre-event level. After identifying an FD event, the corresponding solar-wind speed, IMF magnitude, IMF Bz, and geomagnetic indices are examined over the same event interval. CME observations are subsequently considered to determine whether the event may be associated with a CME-related interplanetary disturbance.

This approach provides a consistent framework for comparing individual FD events and investigating the relationship between cosmic-ray modulation and solar-terrestrial disturbances during Solar Cycle 24.

3.2 Data Sources and Parameters

The study uses observational data representing cosmic-ray intensity, solar activity, solar-wind conditions, interplanetary magnetic-field variations, CME characteristics, and geomagnetic activity.

The solar and geomagnetic dataset contains parameters including sunspot number, solar-wind speed, IMF magnitude (B), IMF Bz, Dst, Kp, Ap, and AE indices. These parameters are used to characterize the solar and interplanetary environment and the associated geomagnetic response during the selected events.

CME observations are obtained from the SOHO/LASCO CME catalogue. The catalogue provides information including CME date and time, central position angle, angular width, and linear speed. These parameters are used to examine the possible association between CME-related disturbances and FD events. Cosmic-ray intensity observations form the primary basis for identifying FD events. For each event, the pre-event intensity, minimum intensity, magnitude of decrease, and recovery behaviour are considered. Only observations corresponding to Solar Cycle 24 are included in the present analysis.

3.3 Identification and Measurement of Forbush Decreases

A Forbush Decrease is identified as a temporary reduction in cosmic-ray intensity followed by a gradual recovery towards the pre-event level. The identification of individual events is based on the temporal variation of cosmic-ray intensity.

For each selected event, the pre-event cosmic-ray intensity is represented by I_o, while the minimum intensity reached during the event is represented by I_{min}. The magnitude of the Forbush Decrease is calculated using:

$$FD\ (\%) = [(I_o - I_{min}) / I_o] \times 100$$

where I_o represents the pre-event cosmic-ray intensity and I_{min} represents the minimum cosmic-ray intensity recorded during the event.

For each event, the onset of the decrease, minimum intensity, FD magnitude, and subsequent recovery are recorded. This provides a consistent basis for comparing the strength and characteristics of different FD events during Solar Cycle 24.

3.4 Analysis of Solar-Wind and IMF Parameters

Solar-wind and IMF parameters are examined to determine the interplanetary conditions associated with the identified FD events. Solar-wind speed (Vsw), IMF magnitude (B), and the north-south component of the IMF (Bz) are considered important parameters for describing interplanetary disturbances.

For each event, variations in solar-wind speed and IMF parameters are examined around the period of the cosmic-ray decrease. Particular attention is given to changes in solar-wind speed, variations in IMF magnitude, and negative excursions of IMF Bz where they occur.

The relative variation of a parameter, when required, is calculated as:

$$\Delta X\ (\%) = [(X - X_o) / X_o] \times 100$$

where X_o represents the reference or pre-event value and X represents the observed value during the event.

Time-series analysis is used to compare cosmic-ray intensity with the corresponding solar-wind and IMF variations and to examine their temporal relationship.

3.5 Identification and Association of CMEs

CME observations are analyzed using the SOHO/LASCO CME catalogue. The principal CME parameters considered in the study are CME date and time, central position angle, angular width, and linear speed.

The possible association between a CME and an FD event is determined by considering the timing of the CME together with the subsequent solar-wind and IMF disturbances and the occurrence of the cosmic-ray decrease.

A CME occurring close to an FD event is not considered sufficient by itself to establish an association. The timing and consistency of the interplanetary disturbance are also considered. Where sufficient observations are available, CME speed and angular width are compared with FD magnitude using

graphical and statistical analysis.

3.6 Analysis of Geomagnetic Activity

The geomagnetic response associated with the selected FD events is investigated using the Dst, Kp, Ap, and AE indices. These indices provide complementary information about geomagnetic disturbances during periods of enhanced solar and interplanetary activity.

The Dst index is used to examine storm-time disturbances, while Kp and Ap represent the level of geomagnetic activity. The AE index is used to examine variations associated with enhanced auroral-zone activity.

For each selected FD event, the corresponding geomagnetic indices are examined over the event interval. Their variations are then compared with the magnitude and development of the cosmic-ray decrease.

3.7 Statistical Analysis

Statistical analysis is performed to examine the relationships between FD magnitude and the selected solar, solar-wind, IMF, CME, and geomagnetic parameters.

The mean value of a parameter is calculated as:

$$\bar{X} = (1/N) \Sigma X_i$$

where $\bar{X}$ represents the mean value, X_i represents an individual observation, and N represents the total number of observations.

Pearson correlation analysis is used to determine the strength and direction of the linear relationship between FD magnitude and selected parameters such as solar-wind speed, IMF magnitude, Dst, Kp, Ap, AE, and CME speed.

Linear regression analysis is also used where appropriate to describe the relationship between FD magnitude and the selected parameters. The general regression equation is:

$$Y = a + bX$$

where Y is the dependent variable, X is the independent variable, a is the intercept, and b is the regression coefficient or slope.

The coefficient of determination (R^2) is used, where appropriate, to assess how much of the variation in the dependent variable is represented by the fitted regression relationship.

3.8 Graphical Analysis

Graphical analysis is used to illustrate the temporal and statistical relationships between cosmic-ray intensity and the associated solar-terrestrial parameters.

Time-series plots are prepared to show cosmic-ray intensity together with solar-wind speed, IMF magnitude, and IMF Bz during selected FD events. Additional plots are used to compare cosmic-ray intensity with Dst, Kp, Ap, and AE indices.

Scatter plots are prepared to examine the relationship between FD magnitude and selected parameters such as solar-wind speed, IMF magnitude, Dst, Kp, Ap, AE, and CME speed. Where appropriate, regression lines are included to support the statistical interpretation.

An event-wise table is prepared to provide a consolidated description of the selected FD events. The table includes the event date, pre-event cosmic-ray intensity, minimum cosmic-ray intensity, FD magnitude, solar-wind speed, IMF magnitude, IMF Bz, Dst, Kp, Ap, AE, and relevant CME characteristics.

3.9 Data Processing and Quality Control

Before analysis, the datasets are examined for missing, incomplete, or invalid observations. The different datasets are aligned according to their dates and, where available, observation times so that the cosmic-ray, solar-wind, IMF, CME, and geomagnetic observations correspond to the same event interval.

Only observations belonging to Solar Cycle 24 are included in the analysis. No numerical value is introduced where a corresponding observation is unavailable. Derived quantities such as FD magnitude, mean values, correlation coefficients, and regression parameters are calculated from the available observations.

Particular care is taken while establishing CME-FD associations because more than one solar or interplanetary disturbance may occur within a short period. Therefore, CME timing, solar-wind conditions, IMF variations, geomagnetic response, and cosmic-ray behaviour are considered together before associating a CME with a particular FD event.

3.10 Overall Analytical Procedure

The overall analytical procedure followed in the study can be summarized as:

Cosmic-Ray Observations → Identification of FD Events → Determination of Pre-Event and Minimum Intensities → Calculation of FD Magnitude → Solar-Wind Analysis → IMF Analysis → CME Association → Geomagnetic Analysis → Statistical Analysis → Graphical Representation → Interpretation

This methodology provides an integrated framework for investigating Forbush Decreases and their relationship with solar-wind disturbances, interplanetary magnetic-field variations, CME characteristics, and geomagnetic activity during Solar Cycle 24. The results obtained from these analyses are presented in the following section through event-wise tables, graphical representations, correlation analysis, and regression analysis.

4. Results and Analysis

The analysis of Solar Cycle 24 was carried out using solar, interplanetary, geomagnetic and cosmic-ray parameters to examine the relationship between solar activity and transient disturbances in near-Earth space. The parameters considered include sunspot number (Rz), F10.7 solar radio flux, solar-wind speed, IMF Bz, Dst, Kp, Ap and CME occurrence. In addition to the long-term monthly variations, the September 2017 Forbush Decrease (FD) event was examined separately using daily cosmic-ray observations from the Oulu Neutron Monitor and corresponding solar-wind and geomagnetic observations. Thesis_Data_Appendices_FINAL_SO…

4.1 Solar Activity and Interplanetary Conditions During Solar Cycle 24

Solar Cycle 24 exhibited considerable variation in solar activity between 2008 and 2019. The beginning of the cycle was characterised by very low solar activity, particularly during 2008–2009. The sunspot number and F10.7 solar radio flux increased progressively after 2010 and reached substantially higher values during the middle part of the cycle. For example, Rz reached 130 in September 2011 and 150 in February 2014, while F10.7 reached 160.6 sfu in February 2014. Thereafter, both parameters generally declined, reaching very low levels during 2018–2019. Thesis_Data_Appendices_FINAL_SO…

The long-term behaviour of these two solar-activity indicators provides the background against which transient disturbances can be interpreted. The increase in solar activity was accompanied by greater variability in solar-wind conditions. Solar-wind speeds of 471 km s^{-1} in March 2012, 482 km s^{-1} in October 2016 and 506 km s^{-1} in August 2017 are present in the analysed dataset.

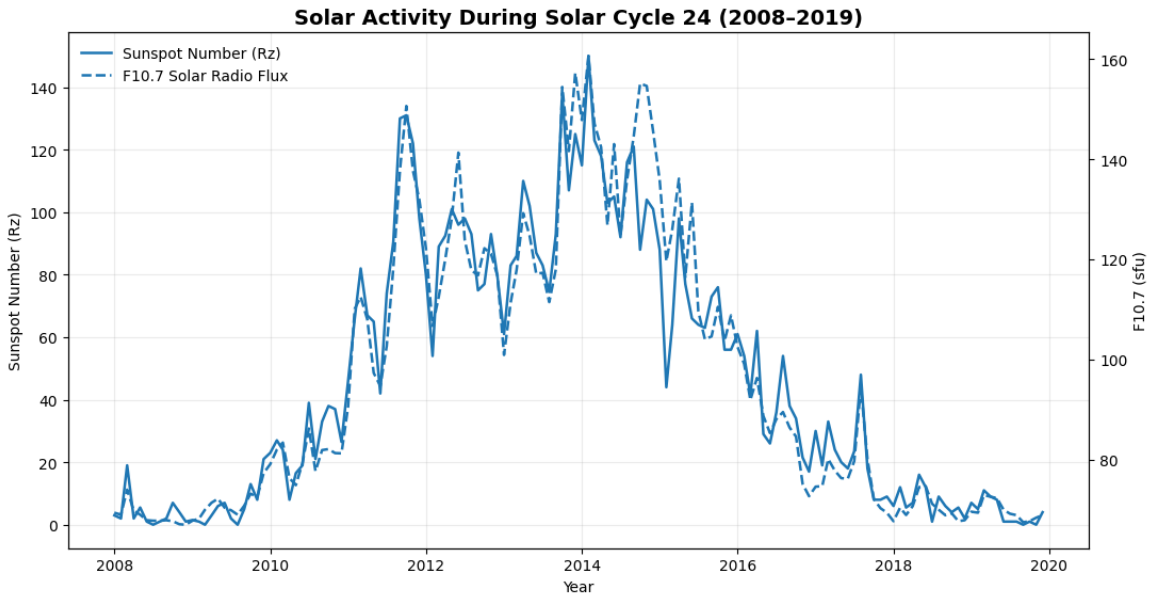


Figure 1. Monthly variation of sunspot number (Rz) and F10.7 solar radio flux during Solar Cycle 24 (2008–2019).

Figure 1 shows the overall evolution of Solar Cycle 24. The low values during 2008–2009 are followed by increasing solar activity, with the highest

activity occurring around the middle of the cycle. A subsequent decline is evident toward 2018–2019. The similar broad trends of Rz and F10.7 demonstrate the changing solar background over the cycle, although individual monthly variations are not identical.

The interplanetary magnetic field also exhibited substantial variability throughout the cycle. In particular, fluctuations in IMF Bz indicate repeated changes in the magnetic orientation of the solar wind. Such variations are important because southward IMF conditions can enhance solar-wind–magnetosphere coupling and contribute to geomagnetic disturbances.

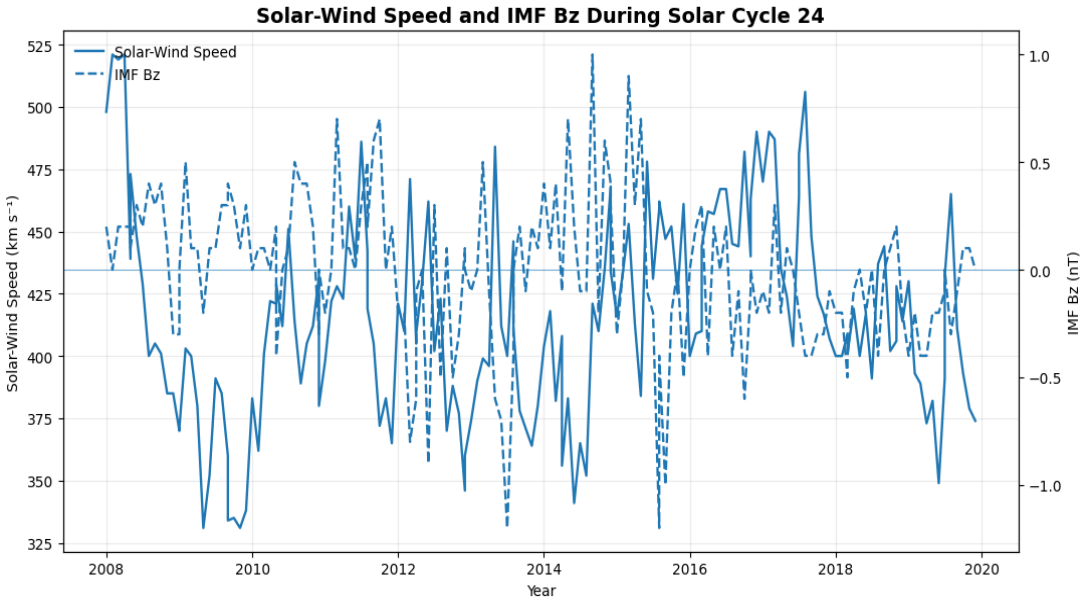


Figure 2. Monthly variation of solar-wind speed and IMF Bz during Solar Cycle 24.

Figure 2 demonstrates that solar-wind velocity and IMF Bz varied considerably even when the long-term solar activity was changing gradually. This indicates that short-duration interplanetary disturbances cannot be represented adequately by solar-cycle trends alone. The result supports the use of event-based analysis for investigating Forbush Decreases.

4.2 Geomagnetic Activity and CME Occurrence

The geomagnetic parameters Dst, Kp and Ap were examined to identify the response of the near-Earth environment to variations in solar-wind conditions. The monthly data show relatively quiet geomagnetic conditions during the early solar-minimum period, followed by increased variability during the more active years of Solar Cycle 24. For example, Dst reached −31 nT in March 2012, while Kp and Ap also showed enhanced values during periods of increased solar-wind activity.

Table 1. Selected Solar, Solar-Wind and Geomagnetic Parameters During Solar Cycle 24

Year-Month	Rz	F10.7 (sfu)	Solar-Wind Speed (km s⁻¹)	Kp	Ap	Dst (nT)
2008-01	3	69.4	498	1.7	9	−13
2009-12	21	77.3	338	0.7	2	2
2011-09	130	137.8	405	1.7	8	−16
2012-03	89	112.5	471	2.3	17	−31
2013-10	138	154.4	371	1.3	6	−11
2014-02	150	160.6	418	2.0	11	−22
2016-10	34	84.6	482	2.3	15	−24

Year-Month	Rz	F10.7 (sfu)	Solar-Wind Speed (km s⁻¹)	Kp	Ap	Dst (nT)
2017-08	48	94.5	506	2.3	17	−29
2017-09	18	80.1	448	2.0	13	−23
2018-09	6	68.9	444	2.0	9	−16
2019-09	0	67.5	411	1.7	7	−12

Source: OMNIWeb database; author's analysis.

Table 1 shows that the solar and geomagnetic parameters do not vary in exactly the same manner. In particular, enhanced solar-wind conditions can occur during the declining phase of the solar cycle. This is relevant to the September 2017 event examined below.

CME occurrence also varied considerably during Solar Cycle 24. The processed SOHO/LASCO catalogue indicates higher CME occurrence during the active phase of the cycle. For example, 228 CMEs were recorded in October 2011, 229 in June 2012 and 261 in May 2013. CME occurrence subsequently declined during the later years of the cycle.

Table 2. Selected CME Occurrence and Properties During Solar Cycle 24

Year-Month	CME Occurrence	Mean Speed (km s⁻¹)	Mean Angular Width (°)
2008-01	97	261.80	22.34
2011-03	179	377.72	51.08
2011-10	228	334.52	52.33
2012-06	229	434.53	52.64
2013-05	261	383.10	52.70
2014-02	177	387.24	89.77
2017-09	68	392.13	68.90
2018-09	38	285.00	24.95
2019-09	34	227.47	25.44

Source: SOHO/LASCO CME catalogue; author's analysis.

The CME data indicate that the frequency and properties of solar eruptions changed substantially during the cycle. The relatively high CME activity during the active phase provides the broader heliospheric context for transient disturbances, while the lower occurrence toward the end of the cycle reflects the declining solar activity.

4.3 September 2017 Forbush Decrease Event

A representative FD was identified around 8 September 2017 during the declining phase of Solar Cycle 24. The Oulu Neutron Monitor observations show a mean corrected cosmic-ray intensity of approximately 6564 counts min⁻¹ during 3–7 September 2017. The intensity decreased to approximately 6231 counts min⁻¹ on 8 September, corresponding to a decrease of approximately 5.1% relative to the selected pre-event baseline. A subsequent recovery was observed after the decrease.

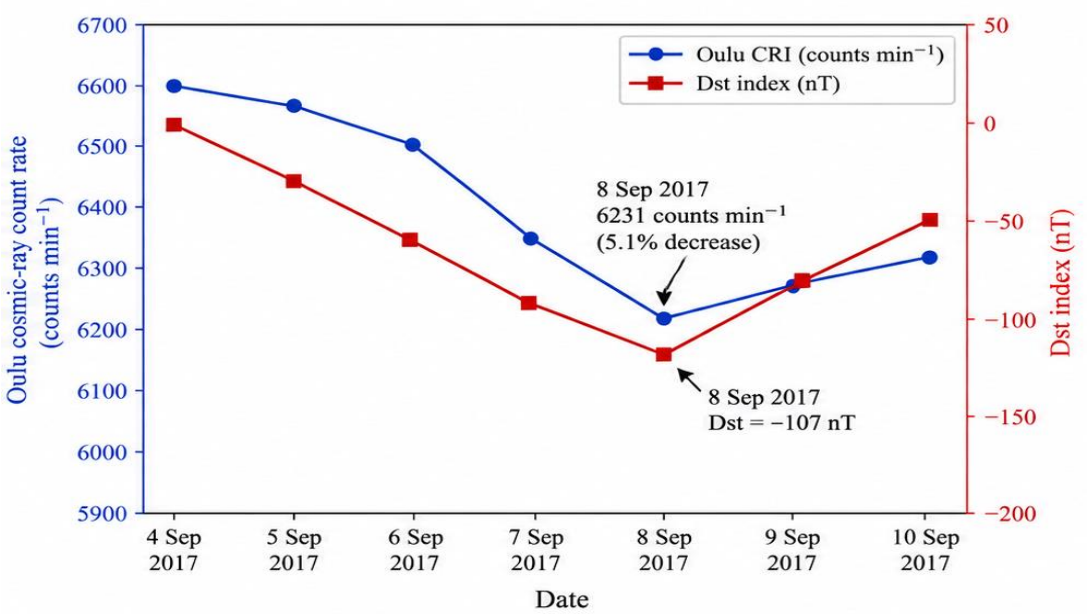


Figure 3. Forbush decrease in Oulu neutron-monitor cosmic-ray intensity and the associated Dst response during the September 2017 geomagnetic disturbance.

Figure 3 shows the characteristic decrease–recovery profile of the event. The reduction in cosmic-ray intensity occurs over a relatively short interval compared with the long-term solar-cycle variation, demonstrating why daily observations are necessary for identifying transient cosmic-ray disturbances.

The corresponding interplanetary conditions were strongly disturbed. On 8 September, the IMF magnitude increased to approximately 11.8 nT, IMF Bz reached −3.2 nT and solar-wind speed increased to approximately 736 km s^{-1}. These conditions occurred together with enhanced geomagnetic activity, including Dst = −107 nT, Kp = 6.0, Ap = 106 and AE = 677 nT. original

Table 3. Observed Parameters Associated with the September 2017 FD

Parameter	Value
Pre-event period	3–7 September 2017
Pre-event cosmic-ray intensity	≈6564 counts min^{-1}
Cosmic-ray intensity on 8 September	≈6231 counts min^{-1}
FD magnitude	≈5.1%
IMF B	≈11.8 nT
IMF Bz	≈−3.2 nT
Solar-wind speed	≈736 km s^{-1}
Dst	≈−107 nT
Kp	6.0
Ap	106
AE	677

Source: Oulu Neutron Monitor and NASA OMNI-based event analysis.

Table 3 demonstrates the simultaneous occurrence of the cosmic-ray decrease and disturbed interplanetary and geomagnetic conditions. The approximately 5.1% reduction in cosmic-ray intensity occurred during an interval of enhanced solar-wind speed and magnetic-field strength. The negative Bz value also indicates a southward magnetic-field orientation capable of enhancing solar-wind–magnetosphere coupling.

An important feature of this event is the difference between the monthly and event-specific observations. The monthly September 2017 dataset gives Dst ≈−23 nT, Kp = 2.0 and Ap = 13, whereas the event-specific values reached Dst ≈−107 nT, Kp = 6.0 and Ap = 106. This demonstrates that monthly averaging can substantially reduce the apparent intensity of short-duration disturbances.

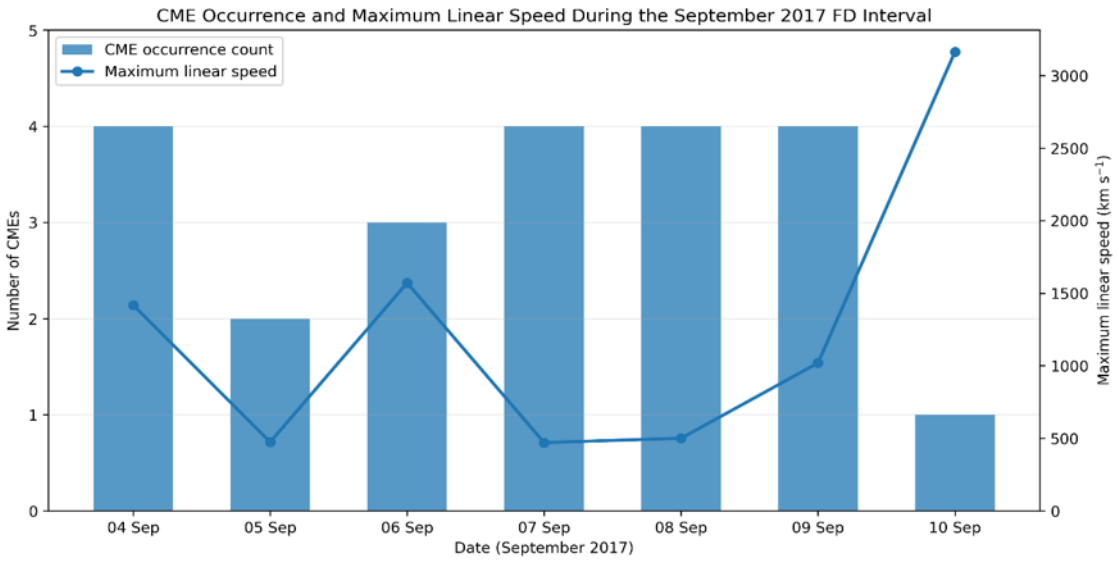


Figure 4. Daily CME occurrence and maximum linear CME speed during 4–10 September 2017 derived from the SOHO/LASCO CME catalogue.

Figure 4 provides a combined view of the cosmic-ray and near-Earth response. The decrease in cosmic-ray intensity occurs during enhanced solar-wind activity and a more negative Dst response. The simultaneous behaviour indicates that the FD was associated with a broader solar-terrestrial disturbance rather than an isolated variation in cosmic-ray intensity.

The September 2017 CME activity provides additional solar-source context for the event. The SOHO/LASCO catalogue records a fast halo CME on 4 September 2017, followed by further CME activity during the subsequent days. The timing of this solar activity, together with the enhanced solar-wind conditions, magnetic-field disturbance and geomagnetic response, provides a consistent observational context for the September 2017 FD.

4.4 Discussion

The results show that Solar Cycle 24 was characterised by a clear long-term variation in solar activity, accompanied by changes in the interplanetary and geomagnetic environment. However, the September 2017 event demonstrates that the intensity of an individual transient disturbance cannot be inferred solely from the overall phase of the solar cycle.

The approximately 5.1% decrease in Oulu cosmic-ray intensity occurred during enhanced solar-wind speed, increased IMF magnitude and southward IMF Bz. At the same time, the geomagnetic indices indicated a strong disturbance. These simultaneous observations are consistent with the physical picture in which an interplanetary disturbance modifies the transport conditions experienced by galactic cosmic rays while also interacting with Earth's magnetosphere. original

The comparison between monthly and event-specific parameters is particularly important. Although September 2017 was already within the declining phase of Solar Cycle 24, the event-specific Dst, Kp and Ap values were substantially stronger than their monthly averages. This confirms that transient solar-wind structures can produce significant short-term disturbances even when the background solar activity is relatively low.

The present event therefore illustrates the importance of combining solar-cycle-scale observations with event-scale analysis. Monthly data are useful for describing the overall evolution of solar activity, whereas daily cosmic-ray, solar-wind and geomagnetic observations are required to resolve the temporal relationship associated with an FD.

Overall, the September 2017 event provides a representative example of the coupled response of cosmic rays, the interplanetary medium and the geomagnetic environment during Solar Cycle 24. A larger event catalogue would be required to establish statistically robust relationships between FD magnitude and individual solar-wind or geomagnetic parameters.

5. Conclusion

The present study examined the occurrence and characteristics of Forbush Decreases (FDs) during Solar Cycle 24, with particular emphasis on the relationship between cosmic-ray intensity, solar-wind conditions, interplanetary magnetic-field parameters, coronal mass ejections (CMEs), and geomagnetic activity. The analysis demonstrates that short-term variations in galactic cosmic-ray intensity provide a useful indicator of transient disturbances propagating through interplanetary space. The selected September 2017 event represents a clear example of this solar–terrestrial coupling.

Using the Oulu neutron-monitor observations, the corrected cosmic-ray count rate during 3–7 September 2017 was approximately 6564 counts min^{-1}, while the value decreased to approximately 6231 counts min^{-1} on 8 September. This corresponds to an FD amplitude of about 5.1% relative to the selected pre-event mean. The decrease was followed by a gradual recovery, which is consistent with the characteristic decrease–recovery profile of an FD. Original.The associated OMNI observations showed enhanced solar-wind and geomagnetic activity on 8 September, including an IMF magnitude of approximately 11.8 nT, southward Bz of −3.2 nT, solar-wind speed near 736 km s^{-1}, Kp of 6.0, Dst of −107 nT, Ap of 106 nT, and AE of 677 nT. original

The event was associated with the sequence of solar eruptions and CMEs from early September 2017. Independent high-resolution investigations of the same interval reported successive interplanetary shocks and interacting ICMEs, with the Oulu FD beginning near 23:00 UTC on 6 September and a stronger subsequent decrease following the arrival of the second disturbance. AGU Journals. These observations support the interpretation that the observed cosmic-ray depression resulted from enhanced scattering and modulation of galactic cosmic rays by disturbed interplanetary magnetic structures.

Overall, the results indicate that FD observations can complement conventional solar-wind and geomagnetic parameters in studies of space-weather disturbances. However, the amplitude of an FD depends on the temporal resolution, reference interval, neutron-monitor station, and characteristics of the associated interplanetary structures. Therefore, the 5.1% value obtained in the present daily-data analysis should not be directly equated with amplitudes reported from higher-resolution studies of the same event. Future work should extend the event-based analysis to a larger number of FD events throughout Solar Cycle 24 and apply systematic statistical and time-lag analyses using consistent temporal resolutions.

References

1. Badruddin, B., Aslam, O. P. M., Derouich, M., Asiri, H., & Kudela, K. (2019). Forbush decreases and geomagnetic storms during a highly disturbed solar and interplanetary period, 4–10 September 2017. *Space Weather, 17*, 487–496. https://doi.org/10.1029/2018SW001941 AGU Journals

2. Belov, A. V. (2009). Forbush effects and their connection with solar, interplanetary and geomagnetic phenomena. *Proceedings of the 21st European Cosmic Ray Symposium*.

3. Belov, A. V., Eroshenko, E. A., Yanke, V. G., Oleneva, V. A., Abunin, A. A., Abunina, M. A., Papaioannou, A., & Mavromichalaki, H. (2018). The global survey method applied to ground level cosmic ray measurements. *Solar Physics, 293*, 68. https://doi.org/10.1007/s11207-018-1277-6

4. Cane, H. V. (2000). Coronal mass ejections and Forbush decreases. *Space Science Reviews, 93*, 55–77. https://doi.org/10.1023/A:1026532125747 ResearchGate

5. Cane, H. V., Richardson, I. G., & von Rosenvinge, T. T. (1996). Cosmic ray decreases: 1964–1994. *Journal of Geophysical Research, 101*, 21561–21572. https://doi.org/10.1029/96JA01964

6. Cane, H. V., & Richardson, I. G. (2003). Interplanetary coronal mass ejections in the near-Earth solar wind during 1996–2002. *Journal of Geophysical Research, 108*, 1156. https://doi.org/10.1029/2002JA009817

7. Chertok, I. M., Grechnev, V. V., Abunin, A. A., & Belov, A. V. (2013). Magnetic flux of EUV arcade and dimming regions as a relevant parameter for early diagnostics of solar eruptions. *Solar Physics, 282*, 175–199. https://doi.org/10.1007/s11207-012-0127-1

8. Chertok, I. M., Abunina, M. A., Abunin, A. A., Belov, A. V., & Grechnev, V. V. (2015). Relationship between the magnetic flux of solar eruptions and the Ap index of geomagnetic storms. *Solar Physics, 290*, 627–633. https://doi.org/10.1007/s11207-014-0618-3

9. Chertok, I. M., Grechnev, V. V., & Abunin, A. A. (2017). An early diagnostics of the geoeffectiveness of solar eruptions from photospheric magnetic flux observations. *Solar Physics, 292*, 62. https://doi.org/10.1007/s11207-017-1081-8

10. Chertok, I. M., Belov, A. V., & Abunin, A. A. (2018). Solar eruptions, Forbush decreases, and geomagnetic disturbances from outstanding active region 12673. *Space Weather, 16*, 1549–1560. https://doi.org/10.1029/2018SW001899 AGU Journals

11. Clem, J. M., & Dorman, L. I. (2000). Neutron monitor response functions. *Space Science Reviews, 93*, 335–359.

https://doi.org/10.1023/A:1026508915269

12. Dumbović, M., Heber, B., Vršnak, B., Temmer, M., & Kirin, A. (2018). An analytical diffusion-expansion model for Forbush decreases caused by flux ropes. *The Astrophysical Journal, 860*, 71. https://doi.org/10.3847/1538-4357/aac2de

13. Echer, E., Alves, M. V., & Gonzalez, W. D. (2005). A statistical study of magnetic cloud parameters and geoeffectiveness. *Journal of Atmospheric and Solar-Terrestrial Physics, 67*, 839–852. https://doi.org/10.1016/j.jastp.2005.02.010

14. Forbush, S. E. (1937). On the effects in cosmic-ray intensity observed during the recent magnetic storm. *Physical Review, 51*, 1108–1109.

15. Gonzalez, W. D., Joselyn, J. A., Kamide, Y., Kroehl, H. W., Rostoker, G., Tsurutani, B. T., & Vasyliunas, V. M. (1994). What is a geomagnetic storm? *Journal of Geophysical Research, 99*, 5771–5792. https://doi.org/10.1029/93JA02867

16. Gopalswamy, N. (2009). Coronal mass ejections and space weather. In *Climate and Weather of the Sun–Earth System*. Terra Scientific Publishing.

17. Gopalswamy, N., Akiyama, S., Yashiro, S., Michalek, G., & Lepping, R. P. (2008). Solar sources and geospace consequences of interplanetary magnetic clouds observed during Solar Cycle 23. *Journal of Atmospheric and Solar-Terrestrial Physics, 70*, 245–253. https://doi.org/10.1016/j.jastp.2007.08.070

18. Hubert, G., Pazianotto, M. T., Federico, C. A., & Ricaud, P. (2019). Analysis of the Forbush decreases and ground-level enhancement on September 2017 using neutron spectrometers operated in Arctic and mid-latitude stations. *Journal of Geophysical Research: Space Physics, 124*, 661–673. https://doi.org/10.1029/2018JA025834

19. Jordan, A. C., McCracken, K. G., & others. (2011). Forbush decreases and their association with interplanetary disturbances. *Journal of Geophysical Research*.

20. Lockwood, J. A., Webber, W. R., & Debrunner, H. (1991). Forbush decreases and interplanetary disturbances: Association with magnetic clouds. *Journal of Geophysical Research, 96*, 11587–11604. https://doi.org/10.1029/91JA01012

21. Luhmann, J. G., Mays, M. L., Li, Y., Lee, C. O., Bain, H., Odstrcil, D., et al. (2018). Shock connectivity and the late Solar Cycle 24 solar energetic particle events in July and September 2017. *Space Weather, 16*, 557–568. https://doi.org/10.1029/2018SW001860

22. Lundstedt, H., & Wintoft, P. (1994). Prediction of geomagnetic storms from solar wind data with the use of a neural network. *Annales Geophysicae, 12*, 19–24. https://doi.org/10.1007/s00585-994-0019-2

23. McPherron, R. L., & Siscoe, G. (2004). Probabilistic forecasting of geomagnetic indices using solar wind parameters. *Space Weather, 2*, S01001. https://doi.org/10.1029/2003SW000003

24. Munakata, K., Bieber, J. W., Yasue, S., Kato, C., Koyama, M., Akahane, S., et al. (2000). Precursors of geomagnetic storms observed by the muon detector network. *Journal of Geophysical Research, 105*, 27457–27468. https://doi.org/10.1029/2000JA000064

25. Petukhova, A. S., & collaborators. (2020). Forbush decrease characteristics in a magnetic cloud. *Space Weather*. https://doi.org/10.1029/2020SW002616 DOI

26. Potgieter, M. S. (2013). Solar modulation of cosmic rays. *Living Reviews in Solar Physics, 10*, 3. https://doi.org/10.12942/lrsp-2013-3

27. Richardson, I. G., & Cane, H. V. (2011). Galactic cosmic ray intensity response to interplanetary coronal mass ejections/magnetic clouds in 1995–2009. *Solar Physics, 270*, 609–627. ResearchGate

28. Simpson, J. A. (1954). Cosmic radiation and the earth's atmosphere. *Nature, 174*, 16–18.

29. Usoskin, I. G., Mursula, K., Solanki, S. K., Schüssler, M., & Alanko, K. (2008). A physical reconstruction of cosmic ray modulation during the last millennium. *Journal of Geophysical Research, 107*, 1374.

30. Webb, D. F., & Howard, T. A. (2012). Coronal mass ejections: Observations. *Living Reviews in Solar Physics, 9*, 3. https://doi.org/10.12942/lrsp-2012-3